Local enzymatic hydrolysis of an endogenously generated metabolite can enhance CPT-11 anticancer efficacy

Zeljko M. Prijovich, Kai-Chuan Chen, and Steve R. Roffler

Institute of Biomedical Sciences, Academia Sinica, Taipei, Taiwan

Abstract

Irinotecan (CPT-11) is a clinically important anticancer prodrug that requires enzymatic hydrolysis by carboxyesterase to generate the active metabolite SN-38. However, SN-38 is further metabolized to inactive SN-38 glucuronide (SN-38G), thus diminishing the levels of active SN-38. Although exogenously administered glucuronide drugs are being investigated for cancer therapy, it is unknown if endogenously generated camptothecin glucuronide metabolites can be used for tumor therapy. Here, we tested the hypothesis that tumor-located hydrolysis of endogenously generated SN-38G can enhance the antitumor efficacy of CPT-11 therapy. EJ human bladder carcinoma cells expressing membrane-tethered β-glucuronidase (EJ/mβG cells) were used to selectively hydrolyze SN-38G to SN-38. Parental EJ and EJ/mβG cells displayed similar *in vitro* and *in vivo* growth rates and sensitivities to CPT-11 and SN-38. By contrast, EJ/mβG cells were more than 30 times more sensitive than EJ cells to SN-38G, showing that SN-38 could be generated from SN-38G *in vitro*. Systemic administration of CPT-11 resulted in tumor-located hydrolysis of SN-38G and accumulation of SN-38 in EJ/mβG subcutaneous tumors. Importantly, systemic administration of CPT-11, which itself is not a substrate for β-glucuronidase, dramatically delayed the growth of EJ/mβG xenografts without increased systemic toxicity. Thus, the anticancer activity of CPT-11 can be significantly enhanced by converting the relatively high levels of endogenously generated SN-38G to SN-38 in tumors. The high concentrations of SN-38G found in the serum of patients treated with CPT-11 suggest that clinical response to CPT-11 may be improved by elevating β-glucuronidase activity in tumors. [Mol Cancer Ther 2009;8(4):940–6]

Received 8/20/08; revised 12/22/08; accepted 1/8/09; published OnlineFirst 4/9/09.

Grant support: Academia Sinica (AS-98-TP-B09), National Health Research Institutes (NHRI-EX94-9420B1), and National Science Council (NSC-95-2311-B001-068-MY3).

The costs of publication of this article were defrayed in part by the payment of page charges. This article must therefore be hereby marked *advertisement* in accordance with 18 U.S.C. Section 1734 solely to indicate this fact.

Requests for reprints: Steve Roffler, Institute of Biomedical Sciences, Academia Sinica, No. 128, Academia Road, Section 2, 11529 Taipei, Taiwan. Phone: 886-2-2652-3079; Fax: 886-2-2782-9142. E-mail: sroff@ibms.sinica.edu.tw

doi:10.1158/1535-7163.MCT-08-0812

Introduction

Camptothecin is an alkaloid anticancer drug isolated from the bark of the South Asian tree *Camptotheca accuminata* (1). Camptothecin selectively binds to and stabilizes topoisomerase I-DNA complexes to kill cells in an S-phase–specific manner (2). Although unsatisfactory results were reported in early clinical cancer trials (3), extensive efforts to improve the pharmacologic properties of camptothecin have resulted in the clinical use of irinotecan (Camptosar, CPT-11) and topotecan (Hycamtin) for more than a decade.

CPT-11 is approved for the first-line therapy of colon cancer (4, 5) and has shown effectiveness in combination therapy and salvage therapy for other malignancies (6, 7). CPT-11, however, possesses little, if any, antitumor activity. Rather, CPT-11 acts as a prodrug that is metabolized in several enzyme-catalyzed reactions (Fig. 1A). Hydrolysis of CPT-11 by carboxyesterase releases SN-38 (8), believed to be largely responsible for CPT-11 antitumor activity (9). In humans, activation of CPT-11 to SN-38 occurs mostly in the liver. SN-38 is an excellent substrate for the detoxifying enzyme UDP-glucuronosyltransferase in the liver, which in turn converts SN-38 to SN-38 glucuronide (SN-38G; ref. 8). Like most glucuronides, SN-38G is a water-soluble, relatively nontoxic metabolite that is removed from the circulation by kidney filtration to urine and by biliary excretion to the upper intestine. Bacterial β-glucuronidase (βG) present in the intestinal tract can hydrolyze SN-38G to release SN-38, causing serious intestinal toxicity and diarrhea, which is one of the dose-limiting side effects of CPT-11 (8). On the other hand, it has been postulated that reabsorption of SN-38 from the intestinal tract may contribute to the prolonged pharmacokinetics of SN-38 and good antitumor activity of CPT-11 (8).

Although CPT-11 displays potent antitumor activity in patients, SN-38 accounts for only 2% to 5% of total drug in the circulation whereas the concentration of SN-38G in the circulation is commonly five or more times higher than SN-38 (10–13). We and others have shown that exogenously administered glucuronide prodrugs can display strong antitumor activity as monotherapeutic agents (14–16), indicating that elevated βG activity found in some tumors may promote the intratumoral activation of glucuronide prodrugs (16, 17). An endogenously generated glucuronide metabolite of aniline mustard also mediated potent antitumor activity against a rat tumor that displayed high βG activity (18). Targeted expression or antibody-mediated accumulation of βG in tumors can also enhance the antitumor activity of exogenously administered glucuronide prodrugs (19–22). Based on these studies, we hypothesized that significant

levels of SN-38G may be present in tumors during CPT-11 therapy and that intratumoral conversion of SN-38G to SN-38 may increase the antitumor efficacy of CPT-11 treatment. Here, we show that tumor-localized expression of membrane-tethered βG can indeed convert an endogenously generated CPT-11 metabolite to a potent anticancer agent, thereby enhancing the antitumor efficacy of CPT-11.

Materials and Methods

Chemicals and Cells

CPT-11, Nuclear Fast Red, H&E, and 5-bromo-4-chloro-3-indolyl β-D-glucuronide were from Sigma-Aldrich. SN-38 was from ScinoPharm. SN-38G was isolated and high-performance liquid chromatography purified from the urine of mice treated with CPT-11. Rat anti-hemagglutinin (anti-HA) monoclonal antibody (mAb) was from Roche. mAb 7G7 (rat anti-mouse βG) has been described (20). Goat anti-rat FITC was from Jackson ImmunoResearch.

EJ human bladder cancer cells (23) were retrovirally infected with pLNCX-mβG-e-B7 as described (20) to express membrane-tethered mouse βG on their surface (EJ/mβG cells). pLNCX-mβG-e-B7 codes for an immunoglobulin κ chain signal sequence, a HA tag [nine-amino-acid peptide sequence (YPYDVPDYA) present in the human influenza virus HA protein], the mature mouse *βG* gene, the immunoglobulin-like C2-type, and immunoglobulin-hinge–like domains of the murine B7-1 antigen followed by the transmembrane domain and cytoplasmic tail of murine B7-1 (20). Cells were cultured in RPMI 1640 supplemented with 10% bovine calf serum in a humidified atmosphere of 5% CO_2 in air at 37°C.

Mice

We used 3- to 4-mo-old Beige-severe combined immunodeficient (SCID) female mice in all experiments. The mice were maintained under specific pathogen–free conditions and fed a standard laboratory diet with free access to food and water, under artificial circadian rhythm. All the experiments using animals were carried out according to United Kingdom Co-ordinating Committee on Cancer Research Guidelines for Welfare of Animals in Experimental Neoplasia (24) and under approval of our institutional animal committee.

Flow Cytometry

EJ or EJ/mβG cells (5×10^5) were stained for 45 min with 0.1 μg rat anti-HA mAb in 50 μL RPMI 1640 or with 5 μg mAb 7G7 in 500 μL RPMI 1640. The cells were washed with RPMI 1640 thrice and incubated for 45 min with 1.5 μg goat anti–rat-FITC in 200 μL RPMI 1640. The cells were washed thrice with medium and 5 μg/mL propidium iodide were added before the fluorescence (excitation 488 nm, emission 530 nm) of 10,000 viable cells was measured on a FACSAdvantage SE (BD Biosciences).

Tissue Sections

Unfixed sections were stained with H&E or incubated for 10 min with 1 mg/mL 5-bromo-4-chloro-3-indolyl β-D-glucuronide in 0.1 mol/L acetate buffer (pH 4.6) containing 5 mmol/L $K_3Fe(CN)_6$ and 5 mmol/L $K_2Fe(CN)_6$. The slides were washed twice with PBS and counterstained for 5 min with Nuclear Fast Red. Slides mounted in GVA mount (Zymed) were examined under an optical microscope (Olympus BX-51).

Enzyme Activity

EJ and EJ/mβG cells or tumor homogenates were assayed for βG activity using *p*-nitrophenol β-D-glucuronide as substrate as described (25).

In vitro [^{3}H]thymidine Incorporation Assay

The pH of EJ or EJ/mβG cell medium was adjusted to pH 6.6 or pH 7.4 by the addition of HCl or NaOH immediately before adding graded concentrations of drugs prepared from stock solutions of 1 mg/mL CPT-11, 1 mg/mL SN-38, or 0.1 mg/mL SN-38G in DMSO. [^{3}H]thymidine (1 μC per well) was measured as described (20).

Intratumoral CPT-11 Metabolites

Beige-SCID mice bearing 150 to 250 mm^3 subcutaneous EJ or EJ/mβG tumors (estimated by 0.5 × length × width ×

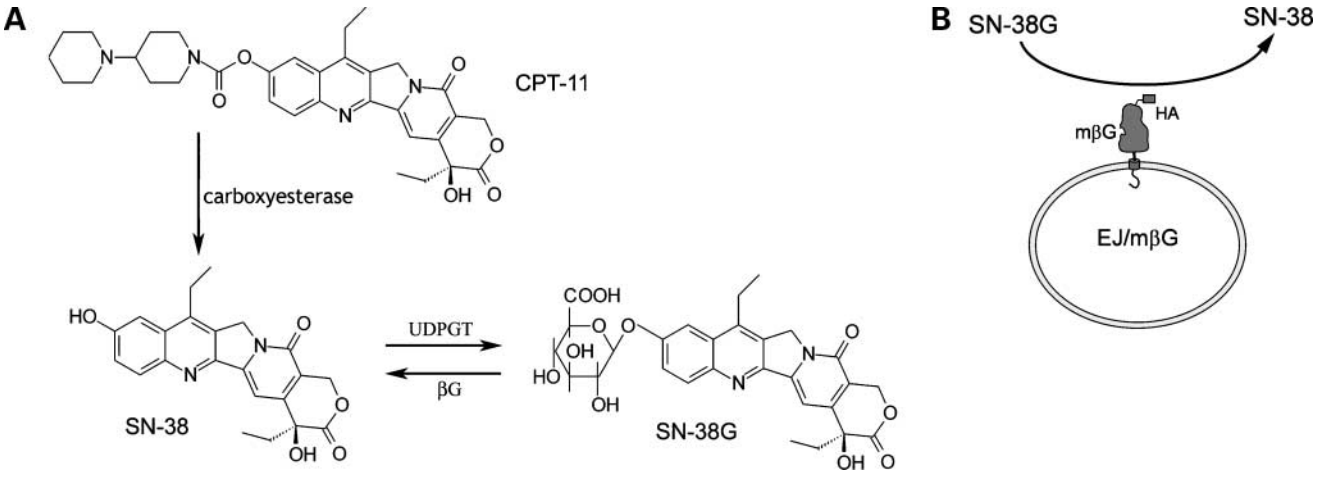

Figure 1. Tumor-located activation of SN-38G. **A**, important phases of CPT-11 metabolism. **B**, schematic of cancer cells expressing membrane-tethered mβG, generated as described in Materials and Methods. A HA tag (YPYDVPDYA) was introduced at the NH_2 terminus of mouse βG.

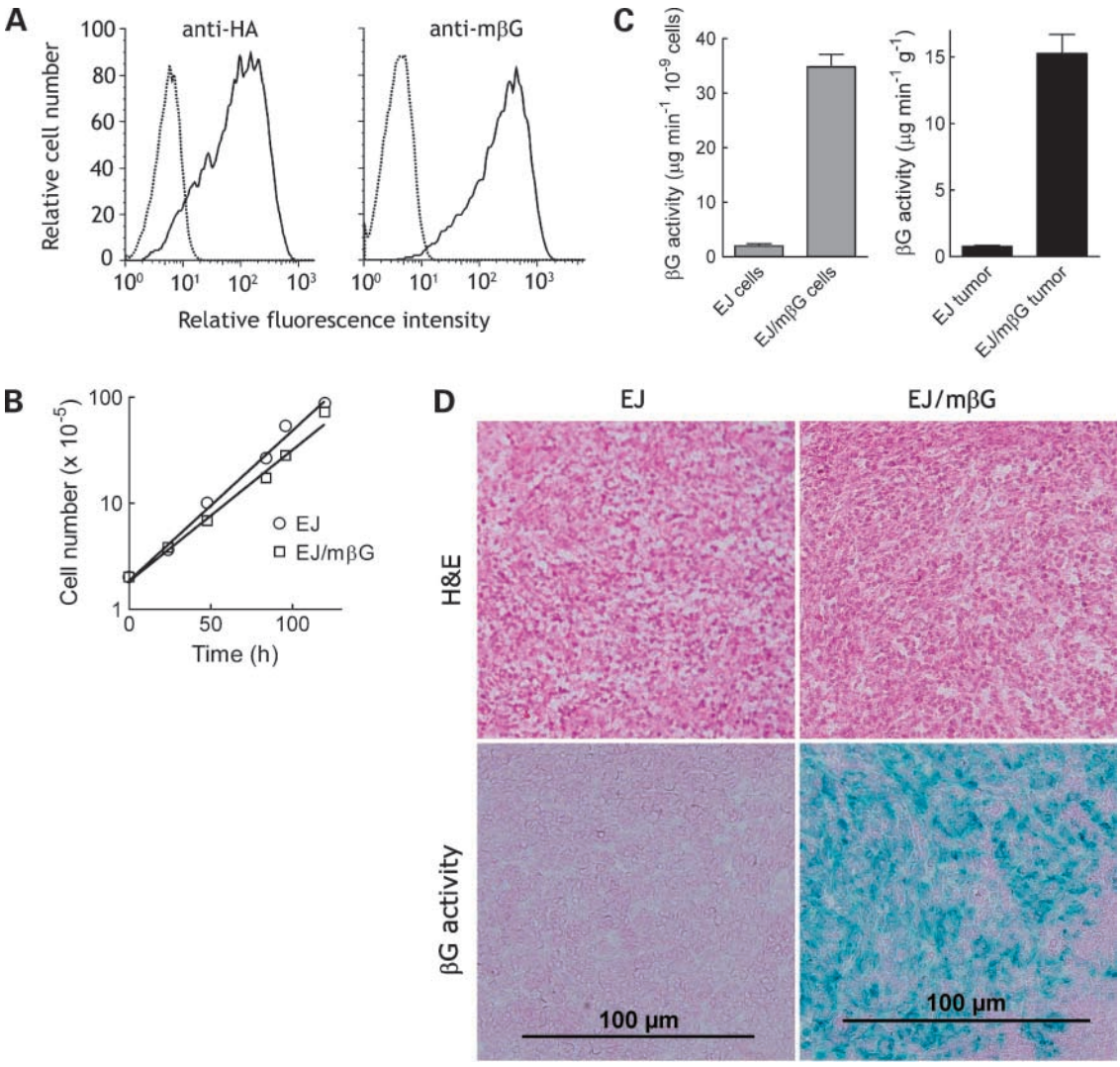

Figure 2. Characterization of EJ/mβG cells. **A,** flow cytometric analysis of mouse βG on EJ cells as determined by immunofluorescence staining with anti-HA mAb (*left*) or anti-mouse βG mAb (*right*). **B,** *in vitro* growth of EJ and EJ/mβG cells. **C,** βG activity of EJ and EJ/mβG cells and tumor homogenates. *Bars,* SD. Differences between βG activity of EJ and EJ/mβG groups were significant ($P < 0.005$). **D,** H&E staining and βG activity in frozen sections of EJ and EJ/mβG tumors.

height) were i.v. injected with 10 mg/kg CPT-11. Blood and tumor samples were immediately dispersed in ice-cold acidic methanol (methanol/water/perchloric acid = 20:20:1) and homogenized for 60 s on an Ultraturax tissue homogenizer at 20,000 rpm. The samples were clarified by centrifugation at 15,000 × *g* for 5 min at 4°C. Supernatants were diluted with 0.1 mol/L KH_2PO_4 and then separated by solid-phase extraction/high-performance liquid chromatography on a μBondapack column with 25% acetonitrile in 0.1 mol/L potassium phosphate buffer (pH 2.9). We detected analytes on a JASCO 2020 fluorescence detector (Jasco) at 375-nm excitation and 430-nm emission for SN-38G and CPT-11 and at 540-nm emission for SN-38. Drugs were quantified by comparison with standard curves generated for drug concentrations ranging from 2.0 pg to 200 ng.

In vivo Antitumor Activity

Groups of Beige-SCID mice bearing ~125 mm^3 EJ or EJ/mβG subcutaneous tumors in their right flank were i.v. injected on 2 consecutive days with 10 mg/kg CPT-11 or PBS. We recorded tumor sizes and body weights for 2 wk.

Statistical Significance

Differences in mean values were analyzed by the independent Student's *t* test for unequal variances. *P* values of <0.05 were considered statistically significant.

Results

Characterization of EJ and EJ/mβG Cells

We engineered EJ human bladder carcinoma cells to express mouse βG on their surface by attaching a linker, transmembrane domain, and cytoplasmic tail to the

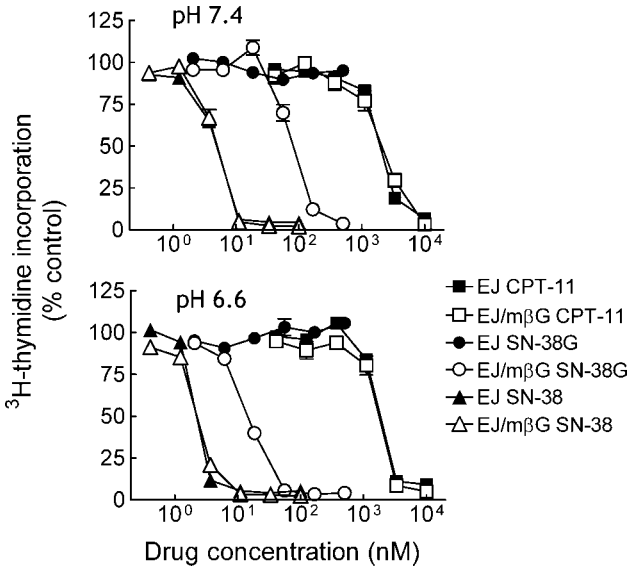

Figure 3. Membrane-tethered βG increases cellular sensitivity to SN-38G. Graded concentrations of CPT-11, SN-38, or SN-38G were added to EJ or EJ/mβG cells at pH 7.4 (*top*) or pH 6.6 (*bottom*) in triplicate for 24 h. The cells were incubated an additional 24 h in fresh medium before cellular incorporation of [^{3}H]thymidine was measured. *Bars,* SD.

COOH terminus of the enzyme (Fig. 1B; ref. 20). Because most glucuronides, such as SN-38G, do not readily cross the lipid bilayer to enter cells, we located βG on the surface of EJ cells to model elevated levels of βG in the interstitial tumor spacer. This models the clinically relevant situations in which interstitial βG activity is naturally high (17) or artificially elevated by antibody (26, 27), gene (20), or bacterial (28) delivery methods. Permanent EJ cells expressing membrane-tethered mouse βG (EJ/mβG) were generated by retroviral transduction of EJ cells. Immunofluorescence staining of live cells with anti-HA or anti-mouse βG antibodies followed by quantification on a flow cytometer confirmed localization of βG on the surface of EJ/mβG cells (Fig. 2A). EJ and EJ/mβG cells grew with similar rates and doubling times of ~24 hours (Fig. 2B), indicating that surface βG did not adversely affect EJ cells. Cultured EJ/mβG cells and tumor homogenates (Fig. 2C) displayed significantly more enzymatic activity than EJ cells or tumor homogenates, verifying that membrane-tethered βG was functionally active. Sections from EJ and EJ/mβG xenografts displayed similar morphologies (Fig. 2D), suggesting that drug penetration into these tumors should be similar. βG activity was also clearly evident on EJ/mβG but not EJ tumor sections as detected by enzyme histochemical staining, confirming that mβG was retained and active on tumors *in vivo* (Fig. 2D). Taken together, these results indicate that EJ/mβG is a suitable and defined model to investigate the effect of intratumoral hydrolysis of SN-38G on CPT-11 therapeutic outcome.

In vitro Cytotoxicity

EJ and EJ/mβG cells were exposed for 24 hours at pH 7.4 or pH 6.6 to graded concentrations of CPT-11, SN-38, or SN-38G. pH 6.6 was examined to investigate the effect of slightly acidic pH, as found in some tumors, on drug cytotoxicity. Cell viability was estimated by measuring [^{3}H]thymidine incorporation into cellular DNA after the cells were cultured an additional 24 hours in fresh medium. As expected for a prodrug, CPT-11 displayed relatively low cytotoxicity to both EJ and EJ/mβG cells with IC_{50} values of ~2,100 nmol/L (Fig. 3). SN-38, by contrast, exhibited potent cytotoxicity against EJ and EJ/mβG cells with IC_{50} values of 6 nmol/L at pH 7.4 (Fig. 3, *top*) and 2 nmol/L at pH 6.6 (Fig. 3, *bottom*). SN-38G was nontoxic to EJ cells at concentrations up to 500 nmol/L. However, EJ/mβG cells were more sensitive to SN-38G with IC_{50} values of 95 nmol/L at pH 7.4 and 16 nmol/L at pH 6.6. Thus, membrane-tethered βG increased the cytotoxic effect of SN-38G to EJ cancer cells.

Intratumoral Distribution of CPT-11 Metabolites

CPT-11 (10 mg/kg) was i.v. administered to Beige-SCID mice bearing established EJ or EJ/mβG xenografts. Tumors were collected and analyzed 2, 8, and 24 hours later. SN-38 levels were 65% to 130% higher whereas SN-38G concentrations were 40% to 50% lower in EJ/mβG tumors compared with EJ tumors (Table 1), demonstrating that membrane-tethered βG converted SN-38G to SN-38 in EJ/mβG tumors. Differences in intratumoral SN-38 and SN-38G drug

Table 1. CPT-11, SN-38, and SN-38G concentrations in EJ and EJ/mβG xenografts in Beige-SCID mice after i.v. administration of 10 mg/kg CPT-11

(Pro)drug	Time (h)	EJ (ng drug per g tumor)	EJ/mβG (ng drug per g tumor)	Difference (%)
CPT-11	2	1,350 ± 200	1,500 ± 230	14.95
	8	87 ± 17	77 ± 178	−10.92
	24	0.58 ± 0.09	0.63 ± 0.11	−8.6
SN-38	2	43 ± 10.5	71 ± 13	65.63*
	8	7.5 ± 0.93	17 ± 5.56	127.10*
	24	0.07 ± 0.02	0.12 ± 0.01	71.43*
SN-38G	2	110 ± 21	62 ± 17	−43.92*
	8	21 ± 5.0	13 ± 1.6	−38.97*
	24	0.32 ± 0.05	0.17 ± 0.01	−46.87*

NOTE: Mean values ± SD of four measurements. Differences are calculated taking EJ values as 100%.
*Statistically significant difference of $P < 0.05$.

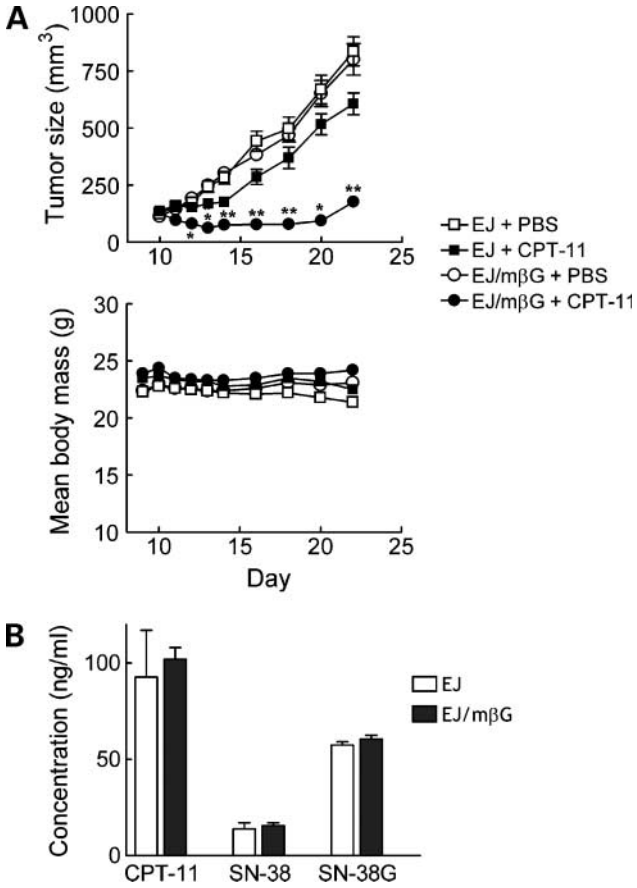

Figure 4. Tumor-located βG can increase CPT-11 antitumor activity. **A,** Beige/SCID mice bearing established EJ or EJ/mβG tumors were i.v. injected with two daily doses of 10 mg/kg CPT-11. Mean tumor size (*top*) and body weights (*bottom*) are shown. *Bars,* SE. Error bars (<10%) are omitted from mean body weights for clarity. Significant differences in EJ/mβG tumor size between mice treated with CPT-11 and PBS. *, $P \leq 0.05$; **, $P \leq 0.005$. **B,** concentration of drugs in the serum of mice bearing EJ or EJ/mβG tumors 2 h after i.v. injection of 10 mg/kg CPT-11. *Bars,* SE.

concentrations were unlikely due to variations in drug exposure because CPT-11 levels were similar in EJ and EJ/mβG tumors.

In vivo Antitumor Activity

Beige-SCID mice bearing established EJ or EJ/mβG xenografts in their right flank were i.v. injected with two daily doses of PBS or 10 mg/kg CPT-11. CPT-11 did not significantly delay EJ tumor growth at this dose. By contrast, CPT-11 significantly delayed the growth of EJ/mβG tumors (Fig. 4A, *top*). Importantly, CPT-11 treatment–associated toxicity, as judged by body mass, did not increase in mice bearing EJ/mβG tumors (Fig. 4A, *bottom*). CPT-11, SN-38, and SN-38G levels in the serum of mice bearing EJ and EJ/mβG tumor were similar at 2 hours after CPT-11 administration (Fig. 4B). Likewise, no significant differences in CPT-11, SN-38, or SN-38G concentrations in mice bearing EJ or EJ/mβG tumors were observed at 8 or 24 hours after CPT-11 administration (results not shown), indicating that tumor-located βG did not affect systemic drug distribution or produce increased levels of SN-38 in the circulation. Thus, tumor-located βG increased the antitumor activity of CPT-11 without obviously increasing systemic toxicity.

Discussion

Although considered a successful drug with more than 10 years of clinical use, CPT-11 efficacy may be hindered by limited conversion of CPT-11 to the active metabolite SN-38 and by subsequent rapid glucuronidation of SN-38 to the inactive glucuronide metabolite SN-38G. Here, we tested the hypothesis that endogenously generated SN-38G is present in tumors at sufficient levels to contribute to the antitumor effects of CPT-11 therapy if it is reconverted to SN-38. As a model system, we used EJ human bladder cancer cells engineered to express membrane-tethered βG on their surface (EJ/mβG cells) to mimic the clinically relevant situations in which interstitial βG activity is naturally high (17) or artificially elevated by antibody, gene, or bacterial delivery methods (19, 20, 22, 26, 28). We found that after CPT-11 treatment, reconversion of endogenously produced SN38G to SN-38 in EJ/mβG bladder tumors significantly enhanced the anticancer efficacy of CPT-11.

The sensitivity of EJ and EJ/mβG cells to CPT-11, SN-38, and SN-38G was investigated at neutral pH (pH 7.4) or at the slightly acidic pH (pH 6.6) found in some tumors (29). Both the cell lines were equally sensitive to CPT-11 or SN-38 *in vitro*. CPT-11 was 400 to 800 times less toxic than SN-38 to both EJ and EJ/mβG cells, in good agreement with previous studies (9). SN-38 was three times more toxic to EJ cancer cells at pH 6.6, likely due to the presence of more active SN-38 lactone at lower pH values (30). The similar sensitivities of EJ and EJ/mβG cells to CPT-11 and SN-38 along with their similar *in vitro* and *in vivo* growth rates and tumor morphologies indicate that membrane-tethered βG did not alter the basic properties of EJ cancer cells.

SN-38G was nontoxic to EJ cells *in vitro* at the highest concentration investigated (500 nmol/L). Glucuronide metabolites are relatively nontoxic because the charged glucuronide moiety hinders drug diffusion across the plasma membrane, thereby preventing access to βG present in lysosomes. Thus, cellular sensitivity to glucuronide drugs correlates with extracellular rather than intracellular βG activity (21). Membrane-tethered βG is accessible to hydrolyze SN-38G to SN-38, resulting in dramatically enhanced

Table 2. Published data of CPT-11 and metabolites in serum after CPT-11 administration in humans

Time (h)	Concentration (ng/mL)			Ratio	Citation
	CPT-11	SN-38G	SN-38	SN-38G/SN-38	
24	80	20	3.5	5.7	(10)
24	60	20	2	10	(11)
24	140	120	4.5	26.7	(12)
6	18	6	1.2	5	(13)

cytotoxicity of SN-38G to EJ/mβG cells with an IC_{50} value of 95 nmol/L at pH 7.4 and 16 nmol/L at pH 6.6. The greater toxicity of SN-38G to EJ/mβG cells at pH 6.6 is likely due to increased SN-38 lactone and greater βG enzymatic activity at acidic pH values (29, 30).

Treatment of mice bearing established tumors with i.v. CPT-11 produced remarkably greater antitumor activity against EJ/mβG tumors compared with EJ tumors. High-performance liquid chromatography measurement of intratumoral drug concentrations found identical levels of CPT-11 in the tumors, verifying similar drug distribution in EJ and EJ/mβG tumors. However, the concentration of SN-38 was 70% to 130% higher and SN-38G was 40% to 50% lower in EJ/mβG tumors than in EJ tumors, showing that specific hydrolysis of SN-38G to SN-38 took place in tumors expressing extracellular βG. This result also emphasizes that SN-38 rather than CPT-11 is responsible for anticancer activity. Although EJ/mβG tumors selectively generated SN-38, SN-38 levels in the circulation were not increased, probably due to the relatively small size of tumors (~0.2 g) compared with the host (~20 g). Thus, preferential intratumoral generation of SN-38 enhanced the antitumor activity of CPT-11 without producing additional systemic toxicity.

The level of serum carboxyesterase responsible for conversion of CPT-11 to SN-38 is higher in mice than in humans, resulting in more rapid systemic hydrolysis of CPT-11 in mice (31). However, in common with mice, SN-38G levels in humans exceed SN-38 levels. SN-38G levels in mice exceeded SN-38 levels by 2- to 4-fold in serum and 2.5- to 4.5-fold in tumors whereas SN-38G levels are 5 to 25 times higher than SN-38 levels in humans (Table 2). Thus, intratumoral hydrolysis of SN-38G to SN-38 may enhance CPT-11 antineoplastic activity even more in humans than in mice.

Our study shows that tumor-located βG may greatly enhance the anticancer activity of CPT-11. Interestingly, antitumor activity was substantially enhanced by increasing the concentration of SN-38 in tumors by only ~2-fold, suggesting that even modest prolonged increases in active drug concentrations can have a relatively large effect on therapeutic outcome. The modest increases in intratumoral SN-38 concentrations in our model case, where enzyme is uniformly expressed on most tumor cells, may indicate limitations of this approach in clinical applications. Potentially beneficial enzyme enrichment by antibody-directed enzyme prodrug therapy/gene-directed enzyme prodrug therapy is expected to be restricted just to a subset of tumor cells, which may limit expected benefits of SN-38G hydrolysis at the tumor site. Previous studies have shown that intratumoral hydrolysis of glucuronide prodrugs can occur in necrotic areas of tumors (17); however, our results indicate that, at least in EJ xenografts, elevation of extracellular βG activity increased SN-38G hydrolysis to SN-38. It should be emphasized that in contrast with therapies in which prodrug is administered to the patient, SN-38G is endogenously generated in patients treated with CPT-11.

Significant amounts of SN-38G remained in EJ/mβG tumors, likely due to the relatively low enzymatic activity of mammalian forms of βG at neutral pH values (20) and possibly due to glucuronidation of SN-38 by UDP-glucuronosyl transferases present in cancer cells (32). Our results suggest that further improvement of CPT-11 therapeutic efficacy can be achieved if additional SN-38G can be hydrolyzed to SN-38 in tumors. It will be important, however, to establish how much βG activity needs to be targeted to tumors to effectively hydrolyze SN-38G as well as to determine the effects of cancer cell UDP-glucuronosyl transferase activity on SN-38 metabolism in solid tumors.

Although methods for efficient enrichment of cancers by βG are still needed, several techniques are under development to preferentially accumulate βG in tumors, including antibody-directed enzyme prodrug therapy (22, 27), gene-directed enzyme prodrug therapy (19, 20), and targeted bacterial expression of *Escherichia coli* βG (28). In addition, mutant human βG enzymes that display enhanced enzymatic activity at neutral pH values are being developed for selective activation of glucuronide drugs in tumors (33). Our study also suggests that selective βG-mediated enhancement of drug activity may be applicable to other anticancer drugs that form glucuronide metabolites, such as epirubicin (34), teniposide (35), flavopiridol (36), and etoposide (37).

In conclusion, we found that during CPT-11 therapy, endogenously produced SN-38G reaches sufficient concentrations in tumors to be intratumorally converted to SN-38 and significantly improve CPT-11 antitumor activity *in vivo* without increasing adverse side effects. High concentrations of SN-38G are also present in patients treated with CPT-11, suggesting that tumor-located expression or targeting of β-glucuronidase is a rational method to improve the antitumor efficacy of CPT-11.

Disclosure of Potential Conflicts of Interest

The authors are potential parties to rewards from Academia Sinica for inventors of licensed technology.

References

1. Wall ME, Wani MC, Cook CE, Palmer KH, McPhail AT, Sim GA. Plant antitumor agents. I. The isolation and structure of camptothecin, a novel alkaloidal leukemia and tumor inhibitor from *Camptotheca acuminata*. J Am Chem Soc 1966;88:3888–90.

2. Hsiang YH, Hertzberg R, Hecht S, Liu LF. Camptothecin induces protein-linked DNA breaks via mammalian DNA topoisomerase I. J Biol Chem 1985;260:14873–8.

3. Gottlieb JA, Guarino AM, Call JB, Oliverio VT, Block JB. Preliminary pharmacologic and clinical evaluation of camptothecin sodium (NSC-100880). Cancer Chemother Rep 1970;54:461–70.

4. Rothenberg ML. The current status of irinotecan (CPT-11) in the United States. Ann N Y Acad Sci 1996;803:272–81.

5. Rougier P, Mitry E. Review of the role of CPT-11 in the treatment of colorectal cancer. Clin Colorectal Cancer 2001;1:87–94.

6. Hakuba N, Hyodo M, Yokoi T, Sato H. Irinotecan (CPT-11) combined with cisplatin for small cell carcinoma of the nasal cavity. Auris Nasus Larynx 2006;33:67–70.

7. Laack E, Thom I, Krull A, et al. A phase II study of irinotecan (CPT-11) and carboplatin in patients with limited disease small cell lung cancer (SCLC). Lung Cancer 2007;57:181–6.

8. Rivory LP. Metabolism of CPT-11. Impact on activity. Ann N Y Acad Sci 2000;922:205–15.

9. Kawato Y, Aonuma M, Hirota Y, Kuga H, Sato K. Intracellular roles of SN-38, a metabolite of the camptothecin derivative CPT-11, in the antitumor effect of CPT-11. Cancer Res 1991;51:4187–91.

10. Poujol S, Pinguet F, Malosse F, et al. Sensitive HPLC-fluorescence method for irinotecan and four major metabolites in human plasma and saliva: application to pharmacokinetic studies. Clin Chem 2003;49: 1900–8.

11. Escoriaza J, Aldaz A, Castellanos C, Calvo E, Giráldez J. Simple and rapid determination of irinotecan and its metabolite SN-38 in plasma by high-performance liquid-chromatography: application to clinical pharmacokinetic studies. J Chromatogr B Biomed Sci Appl 2000;740:159–68.

12. Sparreboom A, de Jonge MJ, de Bruijn P, et al. Irinotecan (CPT-11) metabolism and disposition in cancer patients. Clin Cancer Res 1998;4: 2747–54.

13. Stewart CF, Panetta JC, O'Shaughnessy MA, et al. UGT1A1 promoter genotype correlates with SN-38 pharmacokinetics, but not severe toxicity in patients receiving low-dose irinotecan. J Clin Oncol 2007;25: 2594–600.

14. Houba PHJ, Boven E, van der Meulen-Muileman IH, et al. Distribution and pharmacokinetics of the prodrug daunorubicin-GA3 in nude mice bearing human ovarian cancer xenografts. Biochem Pharmacol 1999;57: 673–80.

15. Angenault S, Thirot S, Schmidt F, Monneret C, Pfeiffer B, Renard P. Cancer chemotherapy: a SN-38 (7-ethyl-10-hydroxycamptothecin) glucuronide prodrug for treatment by a PMT (Prodrug MonoTherapy) strategy. Bioorg Med Chem Lett 2003;13:947–50.

16. Prijovich ZM, Chen BM, Leu YL, Chern JW, Roffler SR. Anti-tumour activity and toxicity of the new prodrug 9-aminocamptothecin glucuronide (9ACG) in mice. Br J Cancer 2002;86:1634–8.

17. Bosslet K, Straub R, Blumrich M, et al. Elucidation of the mechanism enabling tumor selective prodrug monotherapy. Cancer Res 1998;58: 1195–201.

18. Connors TA, Whisson ME. Cure of mice bearing advanced plasma cell tumours with aniline mustard: the relationship between glucuronidase activity and tumour sensitivity. Nature 1966;210:866–7.

19. Heine D, Muller R, Brusselbach S. Cell surface display of a lysosomal enzyme for extracellular gene-directed enzyme prodrug therapy. Gene Ther 2001;8:1005–10.

20. Chen KC, Cheng TL, Leu YL, et al. Membrane-localized activation of glucuronide prodrugs by β-glucuronidase enzymes. Cancer Gene Ther 2007;14:187–200.

21. Cheng TL, Wei SL, Chen BM, et al. Bystander killing of tumor cells by antibody-targeted enzymatic activation of a glucuronide prodrug. Br J Cancer 1999;79:1378–85.

22. de Graaf M, Boven E, Oosterhoff D, et al. A fully human anti-Ep-CAM scFv-β-glucuronidase fusion protein for selective chemotherapy with a glucuronide prodrug. Br J Cancer 2002;86:811–8.

23. Marshall CJ, Franks LM, Carbonell AW. Markers of neoplastic transformation in epithelial cell lines derived from human carcinomas. J Natl Cancer Inst 1977;58:1743–51.

24. Workman P, Twentyman P, Balkwill F, et al. United Kingdom Co-ordinating Committee on Cancer Research (UKCCCR) guidelines for the welfare of animals in experimental neoplasia (second edition). Br J Cancer 1998;77:1–10.

25. Cheng TL, Wu PY, Wu MF, Chern JW, Roffler SR. Accelerated clearance of polyethylene glycol-modified proteins by anti-polyethylene glycol IgM. Bioconjug Chem 1999;10:520–8.

26. Cheng TL, Chen BM, Chan LY, Wu PY, Chern JW, Roffler SR. Poly(ethylene glycol) modification of β-glucuronidase-antibody conjugates for solid-tumor therapy by targeted activation of glucuronide prodrugs. Cancer Immunol Immunother 1997;44:305–15.

27. Chen BM, Cheng TL, Tzou SC, Roffler SR. Potentiation of antitumor immunity by antibody-directed enzyme prodrug therapy. Int J Cancer 2001;94:850–8.

28. Cheng CM, Lu YL, Chuang KH, et al. Tumor-targeting prodrug-activating bacteria for cancer therapy. Cancer Gene Ther 2008;15:393–401.

29. Mürdter TE, Friedel G, Backman JT, et al. Dose optimization of a doxorubicin prodrug (HMR 1826) in isolated perfused human lungs: low tumor pH promotes prodrug activation by β-glucuronidase. J Pharmacol Exp Ther 2002;301:223–8.

30. Prijovich ZM, Leu Y-L, Roffler SR. Effect of pH and human serum albumin on the cytotoxicity of a glucuronide prodrug of 9-aminocamptothecin. Cancer Chemother Pharmacol 2007;60:7–17.

31. Morton CL, Wierdl M, Oliver L, et al. Activation of CPT-11 in mice: identification and analysis of a highly effective plasma esterase. Cancer Res 2000;60:4206–10.

32. Cummings J, Ethell BT, Jardine L, et al. Glucuronidation as a mechanism of intrinsic drug resistance in human colon cancer: reversal of resistance by food additives. Cancer Res 2003;63:8443–50.

33. Chen KC, Wu CH, Chang CY, et al. Directed evolution of a lysosomal enzyme with enhanced activity at neutral pH by mammalian cell surface display. Chem Biol 2008;15:1277–86.

34. Innocenti F, Iyer L, Ramirez J, Green MD, Ratain MJ. Epirubicin glucuronidation is catalyzed by human UDP-glucuronosyltransferase 2B7. Drug Metab Dispos 2001;29:686–92.

35. Rossi C, Zucchetti M, Sessa C, Urso R, Mangioni C, D'Incalci M. Pharmacokinetic study of VM26 given as a prolonged IV infusion to ovarian cancer patients. Cancer Chemother Pharmacol 1984;13: 211–4.

36. Innocenti F, Stadler WM, Iyer L, Ramirez J, Vokes EE, Ratain MJ. Flavopiridol metabolism in cancer patients is associated with the occurrence of diarrhea. Clin Cancer Res 2000;6:3400.

37. Watanabe Y, Nakajima M, Ohashi N, Kume T, Yokoi T. Glucuronidation of etoposide in human liver microsomes is specifically catalyzed by UDP-glucuronosyltransferase 1A1. Drug Metab Dispos 2003;31: 589–95.